British Journal of Haematology, 2003, **120**, 853–859

Pharmacokinetics and red cell utilization of $^{52}Fe/^{59}Fe$-labelled iron polymaltose in anaemic patients using positron emission tomography

Soheir Beshara,[1] Jens Sörensen,[2,3] Mark Lubberink,[4] Vladimir Tolmachev,[4] Bengt Långström,[3] Gunnar Antoni,[3] Bo G. Danielson[5]* and Hans Lundqvist[4] [1]*Department of Clinical Chemistry and* [2]*Department of Clinical Physiology, University Hospital,* [3]*PET Centre and* [4]*Department of Biomedical Radiation Sciences, Uppsala University, and* [5]*Department of Internal Medicine, University Hospital, Uppsala, Sweden*

Received 13 August 2001; accepted for publication 6 February 2002

Summary. Parenteral iron–polysaccharide complexes are increasingly applied. The pharmacokinetics of iron sucrose have been assessed by our group using positron emission tomography (PET). A single intravenous injection of 100 mg iron as iron (III) hydroxide–polymaltose complex, labelled with a tracer in the form of $^{52}Fe/^{59}Fe$, was similarly assessed in six patients using PET for about 8 h. Red cell utilization was followed for 4 weeks. Iron polymaltose was similarly distributed to the liver, spleen and bone marrow. However, a larger proportion of this complex was rapidly distributed to the bone marrow. The shorter equilibration phase for the liver, about 25 min, indicates the minimal role of the liver for direct distribution. Splenic uptake also reflected the reticuloendothelial handling of this complex. Red cell utilization ranged from 61% to 99%. Despite the relatively higher uptake by the bone marrow, there was no saturation of marrow transport systems at this dose level. In conclusion, high red cell utilization of iron polymaltose occurred in anaemic patients. The major portion of the injected dose was rapidly distributed to the bone marrow. In addition, the reticuloendothelial uptake of this complex may reflect the safety of polysaccharide complexes. Non-saturation of transport systems to the bone marrow indicated the presence of a large interstitial transport pool, which might possibly be transferrin.

Keywords: positron emission tomography (PET), ^{52}Fe, ^{59}Fe, iron polymaltose, red cell utilization.

Iron preparations for therapeutic administration include both iron salts and iron hydroxide–polysaccharide complexes. The latter group constitutes formulations for parenteral administration, which have been increasingly applied over the last few years (Macdougall, 1994; Macdougall *et al*, 1996).

Two main concerns have, however, emerged as a consequence of the parenteral application of these complexes, namely, the iron distribution in the different organs, which may be related to late organ damage due to iron accumulation, and the second is the release of free iron that may result in oxidative stress (Figueiredo *et al*, 1993). The rate of iron release from a complex has been suggested to be closely related to the molecular weight of this particular complex. The pharmacokinetics of the individual complexes in terms of iron distribution as well as its availability for marrow utilization need to be further explored.

In earlier studies, the pharmacokinetics and red cell utilization of 100 mg of iron hydroxide sucrose were studied using positron emission tomography (PET) (Beshara *et al*, 1999a,b). Iron (III) hydroxide polymaltose is another polysaccharide iron preparation for intravenous administration with a molecular weight of about 150 kDa.

The aim of the study was to assess the pharmacokinetics and red cell utilization of iron polymaltose by evaluation of the uptake and distribution characteristics of $^{52}Fe/^{59}Fe$-labelled complex, using the PET technique as well as an extended follow-up of radioiron red cell utilization.

PATIENTS AND METHODS

Patients. Six patients (two men and four women), with a mean age ± SD of 45 ± 16 years (range 29–73), were included in the study. Baseline haemoglobin ranged from

Correspondence: Dr Soheir Beshara, Department of Clinical Chemistry, University Hospital, SE-751 85 Uppsala, Sweden. E-mail: soheir.beshara@medsci.uu.se
*Professor emeritus.

Table I. Baseline characteristics of the patients.

No	Age (years)	Sex	Diagnosis	Hb (g/dl)	S-creatinine (μmol/l)	S-Fe (μmol/l)	S-ferritin (μg/l)	TIBC (μmol/l)	TS (%)	rHuEpo therapy dose (U/kg/w)	rHuEpo therapy duration (months)
1	42	f	IDA	11·3	74	7	3·4	74	9·6	–	–
2	35	f	ID	12·4	80	9·7	4·4	88	11	–	–
3	39	m	IDA	10·5	86	3·2	6·1	94	3·4	–	–
4	54	m	Diabetic nephropathy + ID	13·2	266	4·6	178	55	8·4	20	48
5	28	f	Polycystic kidney + RA	10·7	295	20	151	58	34	80	16
6	73	f	Interstitial nephritis + RA	12·5	207	19·4	224	48	40	30	46

S-Fe, serum iron; TIBC, total iron-binding capacity; TS, transferrin saturation; rHuEpo, recombinant human erythropoietin; U/kg/w, unit/kg/week; m, month; IDA, iron deficiency anaemia; RA, renal anaemia; ID, iron deficiency.

10·5 to 13·2 g/dl. Three patients were treated with recombinant human erythropoietin (rHuEpo) at a weekly dose of 20–80 U/kg. None of the patients had received a blood transfusion during the 4 weeks prior to inclusion. Causes of anaemia other than iron deficiency or renal anaemia were excluded and iron supplementation therapy was not allowed during the study. Baseline and clinical characteristics of the patients are described in Table I. The study was approved by the Ethics Committee and the Isotopes Committee of the Medical Faculty of Uppsala University, and informed consent was obtained from all the patients.

Radiopharmaceutical method. The production of ^{52}Fe was performed as described earlier (Beshara *et al*, 1999a).

$^{59}FeCl_3$ was purchased from Amersham (London, UK) in the form of solution in 0·1 mol/l HCl. Before the synthesis of the iron polymaltose, $^{59}FeCl_3$ (in 0·01 mol/l HCl) and $^{52}FeCl_3$ were mixed with a ratio of radioactivity of 1:40, respectively, and the total volume was adjusted to 1 ml. Radiolabelled iron polymaltose was prepared, according to the method developed by Vifor (St. Gallen, Switzerland). Sucrose (100 mg) was dissolved in the iron solution and the pH was adjusted to above 11·8 with 5 mol/l NaOH. Iron polymaltose (2 ml, corresponding to 100 mg of Fe III) was added to this solution. HCl was then added until the pH was between 4·5 and 7 and the solution was filtered through a sterilized 0·22 μm filter into a sterile injection bottle. The injection bolus was diluted to 20 ml using physiological saline and applied over 10 min using a constant volume infusion pump.

The injected positron-derived radioactivity (^{52}Fe/^{52m}Mn) given to the individual patients ranged from 17·4 to 22·1 MBq. The amount of ^{59}Fe was less than 0·5 MBq in all the patients. The effective dose, for the amounts of radioactivity given to the individual patients, was calculated using the model described by Robertson *et al* (1983) and was found to be about a total of 5 mSv for ^{52}Fe and 3 mSv for ^{59}Fe. These levels were approved for this study by the Isotopes Committee of the Medical Faculty.

PET imaging, data acquisition and corrections. PET imaging and data analysis were done as described earlier (Beshara *et al*, 1999a,b). Data analysis was applied in order to obtain standardized uptake values. The PET camera measures radioactivity concentration (Bq/cc). When this is normalized for the injected radioactivity/g body weight, with the assumption that tissue density is 1 g/cc, a ratio value called the standardized uptake value (SUV) is obtained.

The net influx of the radioactivity from blood to tissue as well as the sizes of the reversible pools were analysed using a compartment model; namely blood, reversible and irreversible tissue pools (Rutland, 1979; Patlak *et al*, 1983; Patlak & Blasberg, 1985). The relationship between the tracer concentration in the blood and tissue may be described as follows:

$$C/C_b = V_d + K_t \times T$$

in which $T = \int_0^t C_b(\tau)\,\delta\tau/C_b(t)$.

The time courses of C and C_b (tissue and blood concentration of the tracer respectively) are measured from the tomograms. V_d is the fractional distribution volume of the reversible compartments (no units), t is the real-time following tracer administration (min) and K_t is the transfer rate constant into the irreversible compartment (/min). The integrated part of the equation constitutes the transformed time, which is used to linearize the relationship between tissue and blood concentration. It has a dimension of time as it represents the time integration of the blood curve divided by the blood curve itself. As C/C_b is a ratio between tissue and blood concentration of the tracer, it therefore has no units. According to this model, the intercept of the linear part of the plot represents the distribution volume of the tracer in the reversible compartment and the slope represents the influx constant, which describes the rate of transfer of iron from the blood into the irreversible compartment. This transfer may also be seen as a clearance process, in which K_t represents volume of blood cleared/unit time/volume of tissue.

Radioactivity concentrations were corrected for ^{52m}Mn as described in an earlier study (Lubberink *et al*, 1999).

Radioiron (^{59}Fe) red cell utilization (%)

This was performed as described earlier (Beshara *et al*, 1999a,b), where the red cell utilization (%) was calculated as follows:

Red cell utilization (%) on day n =

WBA/ml on day n/Injected ^{59}Fe radioactivity

× total blood volume (ml) × 100

in which WBA is whole blood radioactivity.

The total blood volume was based on the initial dilution of the administered isotope. A linear regression was applied, using the PET data from the heart, typically between 10 and 30 min, and extrapolated to the time of injection. The PET data were corrected for ^{52m}Mn.

Total blood volume (ml) =

injected activity (Bq)/whole blood radioactivity concentration extrapolated to 0 min (Bq/ml)

The blood-volume values as determined using the PET data from the heart were compared with predicted blood volume calculated from the weights and heights according to the equations described by Nadler *et al* (1962).

RESULTS

PET measurements

The time span of the kinetic studies in the patients ranged from 7·87 to 8·14 h. Changes in the radioactivity concentration in the different tissues over time are shown in Fig 1.

Blood kinetics. Blood kinetics were similar to that of the iron–sucrose complex. However, the blood radioactivity, measured by PET in the left ventricle of the heart, reached values of 13–23% by the end of the study.

Organ uptake. A distribution phase of about 25 min was noted in liver and spleen uptake of iron polymaltose. Standardized uptake values are calculated through normalizing the measured radioactivity concentration (Bq/cc) for the injected radioactivity per gram body weight (Bq/g), with the assumption that tissue density is 1g/cc. A mean liver and spleen uptake of about 27 and 16, respectively, was shown. A slight decrease in liver radioactivity was seen by the end of the PET investigation in all the patients, where the radioactivity reached 55% of the peak value. In patients 4 and 6, an increasing uptake throughout the whole first scanning session, i.e. 85 min, was followed by a slight

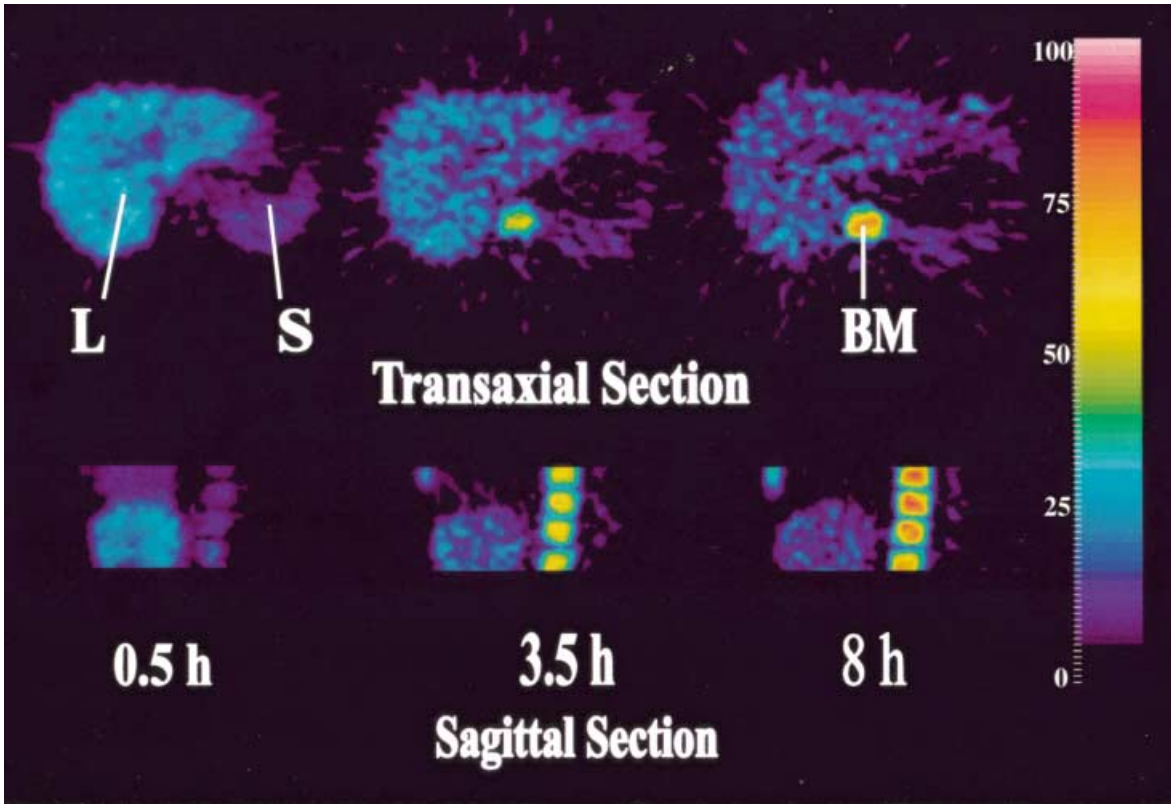

Fig 1. Uptake values of labelled ^{52}Fe-polymaltose in the liver (L), spleen (S) and bone marrow (BM) in one of the patients taken at 0·5, 3·5 and 8 h after injection. The injected radioactivity (Bq) is assumed to be homogeneously distributed all over the body. With the assumption of a tissue density of 1 g/cc, standardized uptake values (SUV) therefore indicate tissue uptake per cc in relation to the injected radioactivity when normalized for the average body uptake per cc. In this patient, maximum radioactivity concentration in BM after 8 h is up to 103 times higher than average body concentration.

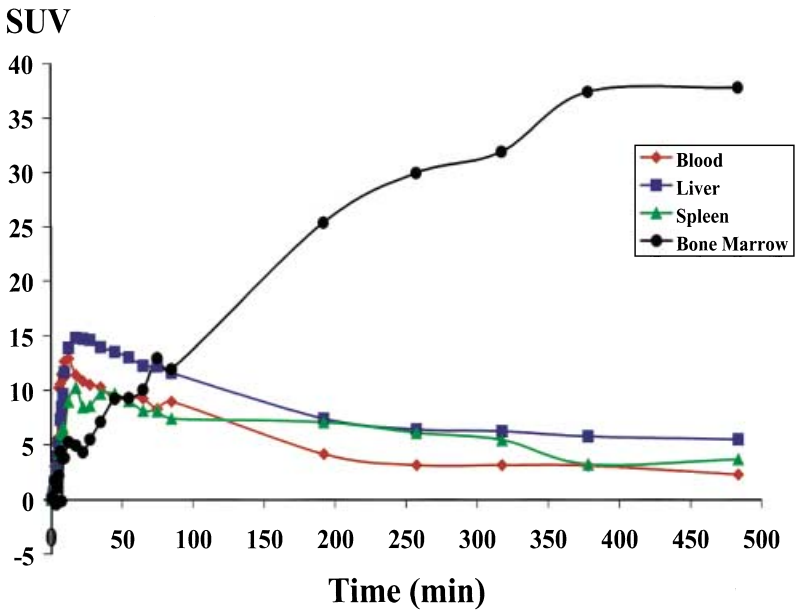

Fig 2. ^{52}Fe-polymaltose uptake curves in the liver, the spleen and the bone marrow in patient 3. Standardized uptake values are presented on the *Y*-axis. These are calculated through normalizing the measured radioactivity concentration (Bq/cc) for the injected radioactivity per gram (g) body weight, with the assumption that tissue density is 1 g/cc. The blood clearance curve is also presented.

decrease towards the end of the study. In the bone marrow uptake curves, a fast radioactivity uptake was seen during the first 10 min followed by an influx of the radioactivity into the bone marrow at a lower but steady rate.

Representative uptake curves in the liver, spleen and the bone marrow in patient 3 are shown in Fig 2.

Graphical analysis. In the bone marrow, no equilibration phase was seen but a straight line was found from the very beginning in all the patients but patient 4. For the liver, the equilibration could be seen after about 20 min, while for the spleen, the equilibration varied in the different patients. The intercepts of the linear part of the liver in the individual patients ranged from 0·55 to 1·33, while that of the bone marrow gave a smaller intercept, which ranged from 0·02 to 0·57. The slopes of the linear part of the regression analysis of the bone marrow reached up to 16 times that of the liver (range 1·9–15·7). Representative linear regression plots in patient 3 are shown in Fig 3.

Radioiron (^{59}Fe) red cell utilization (%)

Predicted blood volumes were within ± 10% of the calculated blood volumes in all patients (Nadler *et al*, 1962).

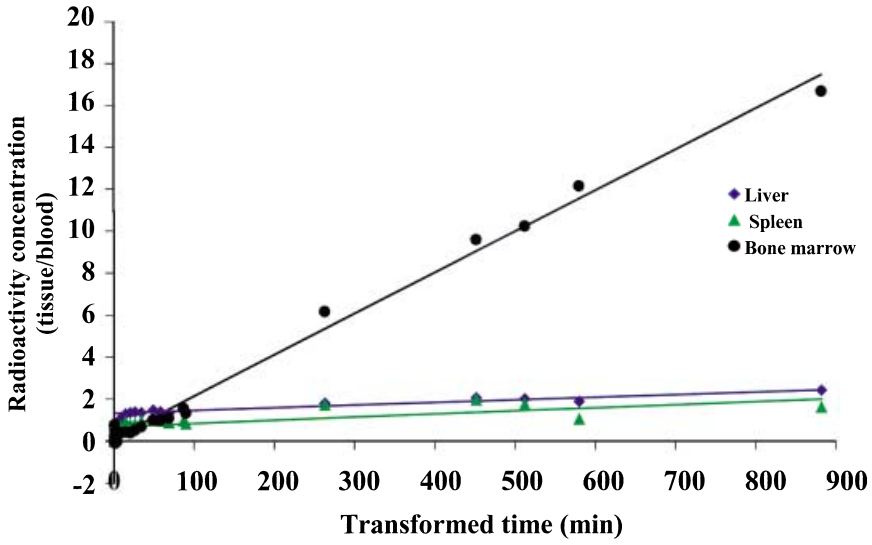

Fig 3. Regression plots in the liver, spleen and bone marrow in patient 3. The radioactivity concentration on the *Y*-axis is a ratio between tissue and blood, and therefore dimensionless, whereas the transformed time on the *X*-axis represents the time integration of the blood–radioactivity curve divided by the blood–radioactivity curve itself. According to the applied compartment model, the intercept of the linear part represents the distribution volume and the slope represents the transfer rate constant from the blood to the irreversible compartment.

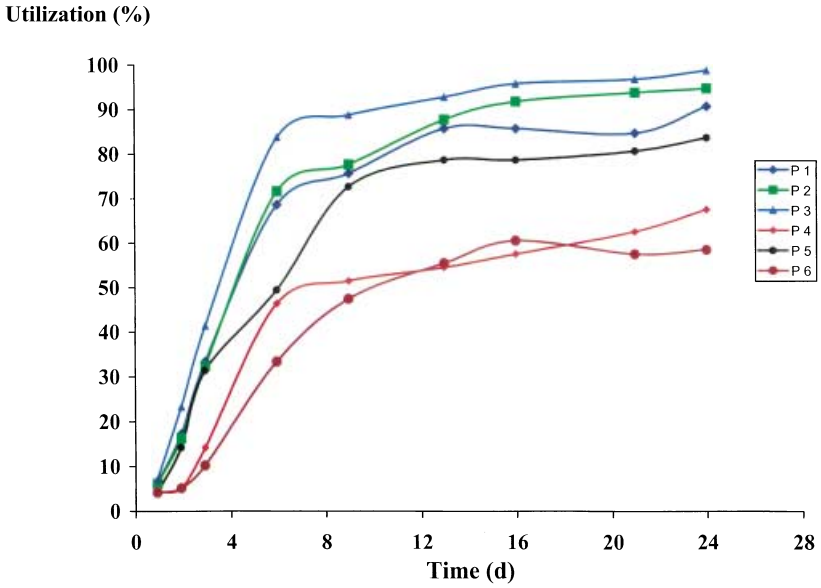

Fig 4. Follow-up data of the rate of ^{59}Fe-iron polymaltose red cell utilization in the individual patients. Day 0 is the day of PET investigation.

The maximum radioiron red cell utilization ranged from 61 to 99% and was reached after 16–24 d. Follow-up data of the rate of red cell utilization in the individual patients are presented in Fig 4.

Changes in Hb levels, reticulocyte counts and iron status

In all the patients but two (patients 4 and 6), Hb levels increased by 1·68 ± 0·8 g/dl (range 0·8–2·4 g/dl) within 2–23 d following administration of the drug. Rapid increase in reticulocyte counts within 1–6 d was noted in patients 1, 2 and 3. In patients 4 and 6, reticulocytosis was noted after 20 and 14 d respectively.

In patients 1, 2 and 3, there was a direct increase in serum (S)-ferritin levels of eightfold to twelvefold above the baseline within 2 d, followed by a decline to baseline levels by the end of the study. Minor changes in S-ferritin levels were noted in patients 4, 5 and 6.

Adverse events

No adverse events were experienced by any of the patients during or following the application of the drug. One patient acquired a haematoma at the site of injection with slowly resolving paresthesia. This was not deemed a drug-related side effect, however, it might be a drug delivery-related side effect.

DISCUSSION

The liver, spleen and bone marrow have been identified as the major pathways for endogenous iron metabolism (Finch *et al*, 1970). The relative distribution of the complex has shown a much higher uptake by the bone marrow in relation to the liver and spleen uptake, compared with the uptake pattern of the iron–sucrose complex.

As the injected iron polymaltose was handled through these organs, a finding which was consistent with the iron–sucrose pattern (Beshara *et al*, 1999a,b), these organs seem to represent the major pathway for the pharmacokinetics of injected iron polysaccharides. Whether the injected iron was taken up by the macrophages or parenchymal cells is of relevance both to its potential toxicity and availability. The uptake by the macrophage-rich spleen of this iron complex, determined by PET technique, was consistent with our observation for the iron–sucrose complex. Such reticuloendothelial uptake of the injected iron polysaccharides was thought to indirectly illustrate the safety of these preparations with regard to the long-term effects on the parenchyma of the various tissues.

The high red cell utilization in the different patients indicated the efficacy of this iron complex. The variation in the percentage red cell utilization was consistent with the observed variations in the early distribution of the complex, as noted in patients 4 and 6.

The increase in S-ferritin levels illustrated the replenishment of the depleted iron stores, which is a well-identified and desired effect of iron therapy.

An interesting observation in this study was that the early distribution to the liver was quantitatively much less for this complex compared with that of the iron–sucrose complex. This, in turn, reflected on marrow uptake, which reached higher levels at earlier time points. The different preparations, although having a similar general distribution pattern, clearly differed in their early distribution components. The early pharmacokinetics of the iron sucrose, molecular weight 43 kDa, involves the liver and spleen as a buffer to a relatively high degree before reaching the marrow, an observation which was not found for the iron polymaltose, molecular weight 150 kDa.

The graphical analysis provided two values, namely the intercept and the slope, which reflected the distribution volume of ^{52}Fe equilibrating with ^{52}Fe in the blood, and the

DOCKET ALARM

Explore Litigation Insights

Docket Alarm provides insights to develop a more informed litigation strategy and the peace of mind of knowing you're on top of things.

Real-Time Litigation Alerts

Keep your litigation team up-to-date with **real-time alerts** and advanced team management tools built for the enterprise, all while greatly reducing PACER spend.

Our comprehensive service means we can handle Federal, State, and Administrative courts across the country.

Advanced Docket Research

With over 230 million records, Docket Alarm's cloud-native docket research platform finds what other services can't. Coverage includes Federal, State, plus PTAB, TTAB, ITC and NLRB decisions, all in one place.

Identify arguments that have been successful in the past with full text, pinpoint searching. Link to case law cited within any court document via Fastcase.

Analytics At Your Fingertips

Learn what happened the last time a particular judge, opposing counsel or company faced cases similar to yours.

Advanced out-of-the-box PTAB and TTAB analytics are always at your fingertips.

API

Docket Alarm offers a powerful API (application programming interface) to developers that want to integrate case filings into their apps.

LAW FIRMS
Build custom dashboards for your attorneys and clients with live data direct from the court.

Automate many repetitive legal tasks like conflict checks, document management, and marketing.

FINANCIAL INSTITUTIONS
Litigation and bankruptcy checks for companies and debtors.

E-DISCOVERY AND LEGAL VENDORS
Sync your system to PACER to automate legal marketing.